Strojniški vestnik - Journal of Mechanical Engineering vol(yyyy)no, p-p
DOI code
Original Paper
Received for review: yyyy-mm-dd
Received revised form: yyyy-mm-dd
Accepted for publication: yyyy-mm-dd

Angstrom-Prescott type models for predicting solar irradiation for different locations in Zimbabwe.

C. Iradukunda[1], and K. Chiteka[2,*]

1 Department of Industrial and Mechatronics Engineering, University of Zimbabwe, P.O. Box MP167, Mt. Pleasant, Harare Zimbabwe.
2 Faculty of Engineering and the Environment, Gwanda State University, P.O Box 30, Filabusi, Zimbabwe E-mail: *tavakudzira@email.com (Corresponding author)

Adequate assessment of solar radiation data is crucial for planning and designing solar energy systems. However, a major challenge facing solar energy technologies is the availability of solar radiation data at the specific area of interest. In this paper solar radiation and sunshine duration data from 29 stations in Zimbabwe were used to generate both monthly and annual Angstrom-Prescott type coefficients, a and b, that are location based. The coefficients were developed using linear correlation between the clearness index and sunshine duration. The adaptation relationship between satellite and ground-measured irradiation had an R^2 of 0.6738. The correlation between the clearness index and the sunshine duration in most of the stations was fairly high with the highest coefficient of determination, R^2, of 0.9030. The Angstrom-Prescott regression coefficient, a, generated using the data from each station ranged between 0.2252 and 0.3976, whereas the regression coefficient, b, ranged between 0.3218 and 0.6265. The estimated and measured values of global solar radiation, H_e, and, H_m, respectively from each station were compared using the mean absolute percentage error (MAPE), the root mean square error (RMSE), the mean absolute error (MAE) and the relative standard error (RSE). The MAE values for the models ranged from 0.5438 MJ/m^2 to 2.2845 MJ/m^2. The MAPE indicated a range between 2.5642 % and 10.334 %. The RSE ranged between 0.0346 % and 0.1537% while the RMSE for the models ranged from 0.7360 MJ/m^2 to 2.9454 MJ/m^2. The statistical indicators showed results that were within the recommended range for solar radiation predicting models from similar studies.

Keywords: Empirical coefficients, Angstrom-Prescott models, Solar irradiation, Sunshine duration.

Highlights:

- Location-specific empirical coefficients from solar radiation data in Zimbabwe were generated.
- Angstrom-Prescott type models for solar irradiation prediction were developed.
- Analyzed model performance and validity using measured data.

0 INTRODUCTION

The world has witnessed substantial negative effects of climate change on water resources, agriculture, biodiversity, human and animal health, forest systems, and socioeconomic sectors [1,2]. Global warming which is somewhat proportional to the increase in the concentration of greenhouse gases (GHG) in the atmosphere, is one of the major observable outcomes of climate change [3,4]. Increased use of fossil fuels in the energy and industrial sectors is considered one of the main causes of the growth in the concentration of greenhouse gases in the atmosphere, particularly Carbon Dioxide (CO_2) [5].

According to scientists, by the end of the current century, global warming may exceed an increase by 4 degrees Celsius [6]. By limiting mean global warming to less than 2.0 °C above preindustrial levels (1850–1900) and pursuing efforts to keep the temperature increase to 1.5 °C, the Paris Agreement was established to proffer a solution (UNFCCC, 2015) to this challenge of global warming. To limit the amount of greenhouse gases released into the environment as a result of burning conventional fuels, the world's energy sector is currently concentrating on encouraging naturally replenished renewable energy sources particularly solar energy [7].

As a desirable replacement for fossil fuels, solar energy is viewed as a natural, sustainable, clean, and ample source of energy that has potential to meet the world's energy needs [8,9]. Many studies have been undertaken to explore this abundantly available sustainable energy source [10,11]. To fully and optimally deploy solar energy, there is need for accurate data to assist in the design and performance analysis of solar energy systems [12]. Over the years the need for accurate and readily available solar radiation data has led to great efforts in development of numerous methods of varying complexity by scientists to estimate solar radiation [13,14]. The various methods developed to forecast solar radiation include stochastic weather models, satellite imaging, linear interpolation, artificial neural networks, physical transfer processes and empirical relations using other meteorological variables [15–19]. For example, recent models have been developed to predict different solar radiation components using different techniques including; machine learning approach with physics-based models, statistical machine learning and numerical models [20–22].

Among prediction methods, the simple empirical models are still being used as the fundamental tool for estimating solar radiation, mainly due to low computation costs, accessibility of data and simplicity [23]. Many solar irradiation predictive models are data driven and hence

classified as empirical. These empirical models are grouped into extensive categories according to their input meteorological parameters such as sunshine duration based models, cloud cover based models, latitude and temperature based models [24]. The main types of empirical models are based on sunshine, temperature and relative humidity [25–27].

Machine learning models have also been used in predicting solar radiation. These are trained artificial systems that combine various meteorological input variables like sunshine duration, temperature, relative humidity and cloud cover from both satellite imaging and ground measurements to predict solar radiation [28]. Robust linear regression, support vector machines, artificial neural networks, extreme gradient boosting (XGBoost), and random forests are some of the machine learning models that have recently emerged as sophisticated methods for constructing more precise correlations between inputs and outputs [29–33]. Machine learning models perform well when estimating solar irradiation, but their ease of use and transferability from the development site to the intended areas is totally dependent on the geographic and climatic condition [26]. ARIMA-GP evolutionary models were recently developed by Nwokolo et al. [20,21] and these were found to be sufficiently accurate in the prediction of solar irradiation in different locations.

Many other attempts have been made to develop models to predict solar irradiation. For example, Sabbagh et al. (1977) proposed a model for use in dry arid or semi-arid regions, such as Iran, where the average sea level is higher. The model considered the effect of relative humidity (RH), and maximum temperature (T_{max}) on solar radiation. Kasten and Czeplak [35] developed a cloud cover based model that correlated the ratio of global solar radiation (H) to the total amount of cloud cover and global radiation at cloudless sky (H_o). Nwokolo [36] performed a comprehensive review of empirical models used for estimating global solar radiation in Africa and West Africa. The study indicated that hybrid models performed better than single-parameter based models in the prediction solar radiation. In a different study, Nwokolo and Ogbulezie [37] undertook a quantitative review and classification of empirical models used for predicting global solar radiation in West Africa. The study recommended the need to make use of soft computing as an alternative approach to estimating global solar irradiation with high precision in West Africa.

Temperature based models are also popular and some of these assume that the difference between the maximum and minimum temperature is directly linked to solar radiation received at the surface [38]. Bristow and Campbell [39] proposed a temperature based model that relates solar irradiation to maximum and minimum temperature cognisant of the transmissivity of the atmosphere. In a different study, Donatelli and Campbell [40] devised a model that takes into account the average air temperature and minimum temperature functions, as well as the atmosphere's transmissivity coefficient to predict solar radiation. A study by Nwokolo et al. [41] investigated a single hybrid parameter-based model for optimizing the Hargreaves-Samani coefficient in Nigeria. The study indicated that the same approach could also be applied in the prediction of global solar radiation.

Sunshine duration-based models have been found to be equally important and applicable to solar irradiation prediction. The Angstrom-Prescott model is the first linear correlation relating solar radiation to sunshine duration and is the most commonly employed model for predicting global solar radiation as a result of availability and reliable sunshine duration measurements in most meteorological stations [42]. Many modifications of this model have been proposed in literature. For example, the Glover and McCulloch Model which is a modification of the Angstrom-Prescott model further incorporate the latitude into the linear Angstrom-Prescott model [43]. Likewise, the modified Angstrom-Prescott model established by Page [44] is considered a model that can be used anywhere in the world; however, it should be noted that it was developed for a latitude of 40 degrees, thus it is preferable to recalculate the correlation coefficients of, a and b, [26,45,46].

The Bahel model is also based on sunshine duration and is a relationship between sunshine duration and solar radiation data obtained from 48 weather stations around the world, under various geographical and meteorological conditions [47]. On the other hand, Dehkordi et al. [48] developed modified coefficients of the Angstrom-Prescott model for six meteorological stations across the arid and semi-arid regions of Iran. The study generated Angstrom-Prescott models for each station using meteorological data recorded from 1992 to 2017.

Mostafazadeh et al. [49] developed two modified Angstrom-Prescott models for predicting solar radiation using both sunshine duration and solar radiation data from Urmia and Tabriz stations in Iran from the period of 2014 to 2017. In order to evaluate the models' accuracy the study employed Root Mean Square Error, Mean Absolute Bias Error and Nash-Sutcliffe Efficiency indices. The statistical analysis of the models indicated that the modified models of Urmia and Tabriz stations produced very good prediction values. The conclusion was that since sunshine duration is an important variable for estimating solar radiation then the modified Angstrom-Prescott models can be used to predict solar radiation in Iran [48,49]. Mejia et al. [50] developed an algorithm for predicting solar radiation in Ciudad Juarez Chihuahua, Mexico based on a modified Angstrom-Prescott model. The modified prediction model was developed using data from NASA's World Energy Resources forecast database for Ciudad Juarez, Chihuahua, including daily average radiation and sunlight duration.

Lewis, [46] used two empirical models to estimate solar irradiation over Zimbabwe using measured data from a station based in Harare. The first model was a correlation between clearness index and the fraction of sunshine hours based on the Angstrom-Prescott model and the second model was based on a linear correlation between clearness index and maximum temperatures and Relative Humidity. The study generated correlation coefficients for the first model and used similar data from Nigeria by Swartman and Ogunlade [52], then generated correlation coefficients for the second model and used similar data from Iran by Sabbagh et al [34] to test and analyse the applicability of both models. The analysis concluded that the first model based on sunshine duration data was the better of the two models as it estimated solar radiation values that were close to the measured values. The study also concluded that the use of the first model to predict solar irradiation over Zimbabwe was less accurate as only data from Harare was used to generate the model, hence the study recommended the use of data from other stations across Zimbabwe to generate more location specific models which

would perform much better than a model based on data from a single location.

Chagwedera and Sendezera [53] developed two correlation models of the Angstrom type to predict the monthly average daily global solar radiation incident on a horizontal surface using meteorological data from two locations (Bulawayo and Harare) in Zimbabwe. The study used the models to generate estimated solar radiation values which were compared to measured solar radiation data. The results showed good agreement between measured and predicted solar radiation values and the authors concluded from the findings that modifying the Angstrom type model to generate location-based models produces improved solar radiation predictions.

Chiteka and Enweremadu [54] developed an artificial neural network model for predicting horizontal irradiation for important sites in Zimbabwe, which included a seven input layer, one hidden layer, and a single output layer. The inputs of the neural network developed by the authors consisted of geographical data of altitude, latitude and longitude and meteorological data of humidity, pressure, clearness index and average temperature. The best predictive model of all the models studied was a network with 10 neurons and a tansig transfer function in both the input and output layers. The network had a coefficient of determination of 99.894 %, a root mean square error of 0.223 kWh/m^2/day, a mean absolute error of 0.17 kWh/m^2/day, and a mean absolute percentage error of 2.56 percent, according to the evaluations.

The Angstrom-Prescott model is an economic, meteorological and geographic empirical model that has been applied in different locations around the world to predict the proportion of solar irradiation incident on the horizontal surface in all sky conditions anywhere on the globe [26,38]. Studies agree on its simplicity and remarkable performance due to the strong correlation between sunshine duration and solar radiation. Despite its low performance compared to machine learning models, it is a powerful hybrid estimation technique, and this attribute gives the Angstrom-Prescott model an advantage or preference over other linear and nonlinear functional forms to improve the accuracy of the model's performance, making it a reference model.

Understanding and measuring the solar radiation's spatial-temporal distribution is crucial for optimizing solar energy harvesting in many applications. At numerous meteorological stations and individual weather stations, measurements of solar radiation are taken on the ground using two different types of instruments i.e a pyrheliometer and a pyranometer. Adequate assessment of solar radiation data is crucial for planning and designing solar energy systems [55]. However, a major challenge facing solar energy technologies is the availability of solar radiation data at the specific area of interest. There are three main ways in which this deficiency in solar radiation data manifests itself: low spatial coverage, a short record and a lack of both global radiation data and sunshine duration [56]. The shortage of solar radiation data arises as a result of a finite number of observation stations mainly due to financial and technical limitations especially in developing countries [16].

In Zimbabwe station-based meteorological solar radiation data still remains scant as there is only a few weather stations that measure solar irradiation. At these stations data recording on solar irradiation is measured by pyranometers and is monitored by the Meteorological Services Department (MSD) [57]. Pyranometric measurements are difficult to obtain due to high costs of setting up the measuring equipment. This unavailability of measured solar irradiation data in developing countries is a major limitation when assessing solar energy potential in various areas [58]. As a result, a continual mapping of solar radiation via estimation is required [56].

Solar radiation at the surface of the earth is a complex parameter to accurately estimate due to varying weather conditions across the globe, therefore this limits the Angstrom-Prescott model to a location specific model. The Angstrom-Prescott model's accuracy can be enhanced by introducing into the initial model, site specific meteorological data and parameters [50]. It is against this background that models are developed based on the Angstrom-Prescott model for predicting solar irradiation specific for the environment in Zimbabwe. In many studies in which the different empirical models have been compared, it has been observed that the sunshine duration based models perform better than the other empirical models and most of the sunshine based models generated to estimate solar radiation are modifications of the Angstrom-Prescott model [59]. As such, the model has become a reference and fundamental model for estimating solar radiation in any location in the world.

Meteorological stations in Zimbabwe that measure and record ground solar radiation are sparsely distributed over a landscape with dynamic climate and weather shifts. Furthermore, the solar radiation data available at the few stations in Zimbabwe is historical data ranging between 1975 to 1999, hence it is not applicable to current solar radiation research as the data does not incorporate atmospheric changes that have occurred over the years. Solar radiation data from solar resource maps and spatial solar radiation data sets is more consistent than the ground measured data but its limitation is that the data is less accurate due to exclusion of atmospheric impact on solar irradiation received on the ground. The use of outdated and/or less accurate solar data from the meteorological stations and satellite database results in overestimation or underestimation of both research and design outputs which can affect the financial decisions of solar radiation-based projects and research significantly. Moreover, geostationary satellites often have no coverage in some areas on the globe [60] and hence various authors have tried to overcome this drawback by correlating the satellite derived data with corresponding ground measurements, thus generating a correction factor for the satellite data.

It is therefore imperative to develop a solar irradiation predicting model adapted from the consistent satellite data and both current and historical ground measured solar radiation data specific to the environment in Zimbabwe. Developing a solar radiation predicting model based on the Angstrom-Prescott model will reduce the need to establish expensive solar radiation measuring equipment since the solar irradiation will easily be estimated by the model. In this study, location-specific empirical coefficients were generated from solar radiation data from locations in Zimbabwe. This was followed by developing an Angstrom-Prescott model for estimating solar irradiation. The model was analysed and validated for its applicability by comparing with measured data. The rest of this study is structured as follows; section 1 focuses on the materials and methods used in the study while section 2 outlines the results and discussion of the results. Section 3 highlights the major conclusions of the study.

1 METHODOLOGY

1.1 Study location

Zimbabwe is a landlocked country in the Southern part of Africa surrounded by countries like Zambia in the north, South Africa in the south, Botswana in the west and Mozambique in the east. This country is located in the tropics between latitude 15.61˚S – 22.42˚S and longitude 25.24˚E – 33.05˚ E [65]. The climate is subtropical in general, however, it may be divided into five distinct climatic zones according to the Koppen-Geiger classification [66]. The north and east (the Low veld) are particularly warm and wet, and are classified as humid and subtropical, with a highland zone in the centre-east. In the shadow of the eastern highlands, the high elevation plateau in the west (the Highveld) experiences milder temperatures and is protected from rain, resulting in a climate that is closer to semi-arid. This semi-arid zone stretches from the country's southernmost point to the southeast, where a tiny area of near-desert conditions exists [66].

1.2 Meteorological Datasets

The data sets used comprised of three different data sources including ground measurements from 29 meteorological stations in Zimbabwe, measurements from a University of Zimbabwe observation station as well as solar radiation satellite-based observational data obtained from NASA POWER Data Access (https://power.larc.nasa.gov/data-access-viewer/) website. Historical pyranometer measurements of monthly mean solar radiation measurements were obtained from the Meteorological Service Department (MSD). The data range was from January 1971 to June 2000 but only nineteen of the 29 stations measured monthly solar radiation. Recent ground measured monthly solar radiation data from 2006 to 2020 was also obtained from a mini-meteorological station at the University of Zimbabwe Physics Department.

Satellite-based global solar radiation data on a horizontal surface for the 29 stations over a period of 15 years (2006-2020) was also obtained from NASA POWER Data Access. These datasets are enhanced meteorological datasets developed with the Goddard Earth Observing System (GEOS) atmospheric model and Data Assimilation System (DAS) with a spatial resolution of 0.5° longitude and 0.5° latitude [27,67,68]. The datasets have been used over the years in many studies where ground measurements are not available, to obtain daily global solar radiation data [61,69]. The monthly average sunshine duration measurements recorded by sunshine recorders was obtained from the MSD for the 29 meteorological stations in Zimbabwe from the period of 1971 to 2020.

1.3 Satellite data correction

The evaluation of satellite data performance has been found to possess significant biases, which can be attributable to potential errors in the satellite data measurements of ground parameters due to changes in tropospheric features and surface environmental conditions as well as measuring methods [70–73]. Hence, applying a correction factor to satellite-derived data in order to obtain corresponding ground based measurements results in a comprehensive solar radiation database [62,63,74].

The mini-station at the University of Zimbabwe Physics Department was the only station with recently recorded monthly ground measurements of solar radiation from the year 2006 to 2020. Therefore the ground measured data at the mini-station were used to calibrate the satellite-based measurements in order to make the data sets compatible through a correlation plot between ground-based and satellite-based solar radiation measurements.

1.4 Meteorological Parameters

The computation of the extra-terrestrial solar radiation (H_o) is shown in Eq. (1) as a function of the latitude (φ) [75].

$$H_o = \frac{24\times 3600}{\pi}\times I_{sc}\times E_o\left[\frac{\pi}{180}\omega_s \sin\varphi\sin\delta + \cos\varphi\cos\delta\sin\omega_s\right] \quad (1)$$

The solar constant, I_{sc}, is the energy from the sun per unit time received on a unit area of a surface perpendicular to the direction of the radiation at the mean Earth-Sun distance outside the atmosphere and is given by 1367 W/m^2 as adopted by the World Meteorological Organisation [76]. E_o, is the relative earth-sun distance or the eccentricity correction factor of the earth's orbit and its value is given by the Eq. (2) where n is the day of the year starting from 1 to 365 and 366 on a leap year [77].

$$E_0 = 1 + 0.033\times\cos\frac{360n}{365} \quad (2)$$

The solar declination angle, δ, and the sunset hour angle, ω_s, are computed using Eqs. 3 and 4 respectively [78].

$$\delta = 23.45\sin\left[360\left(\frac{284+n}{365}\right)\right] \quad (3)$$

$$\omega_s = \cos^{-1}\left(-\tan\delta\tan\varphi\right) \quad (4)$$

The maximum possible sunshine duration in hours is given by Eq. (5) [75]:

$$S_o = \frac{2}{15}\omega_s \quad (5)$$

H_o, and, S_o, where thus computed using Eq. (1) and (5) respectively per station for each month and their averages per station are shown in Table 1.

Table 1. *Computed meteorological parameters for selected locations*

Station	Lat. (º)	Elevation (m)	S (Hours)	S_o (Hours)	S/So	H (MJ/m^2)	H_o (MJ/m^2)	H/H_o
Beitbridge	-22.22	457	8.503	11.998	0.7135	21.319	33.774	0.6380
Grand Reef	-18.98	1019	8.193	11.998	0.6878	21.234	34.406	0.6529
Gweru	-19.45	1429	8.316	11.998	0.7001	22.301	34.318	0.6638
Mt Darwin	-16.78	953	8.209	11.998	0.6900	21.696	34.781	0.6383
Nyanga	-18.22	1679	7.675	11.998	0.6458	21.250	34.541	0.6288
Victoria Falls	-17.93	1062	8.890	11.998	0.7494	24.075	34.590	0.7107

1.5 Data quality control

The data for modelling was reliant on solar radiation and sunshine data and therefore it was imperative to check the quality of both ground and satellite-based data in order to minimise errors in the models. The scatter envelope technique was used to check the quality of data between the clearness index, H/H_o, and the fraction of the sunshine duration, S/S_o. The scatter envelope technique is a statistical method that quantifies the boundaries and number of data outliers using standard statistics such as standard deviations and averages [79]. The input data were the fraction of sunshine duration and the clearness index, therefore the clearness index was divided into ten equal bands, each with a fraction of sunshine duration value of 0.1. In each band, the standard deviation, σ, and mean value of the clearness index, H/H_o, shown in Fig. 1. were assessed, and the dispersion envelope was defined by the limits ($H/H_o \pm 2\sigma H/H_o$). The dispersion envelope is the area bordered by the two curves that represent the upper and lower bounds, with the higher limit representing ($H/H_o + 2\sigma H/H_o$) and the lower limit representing ($H/H_o - 2\sigma H/H_o$) [80].

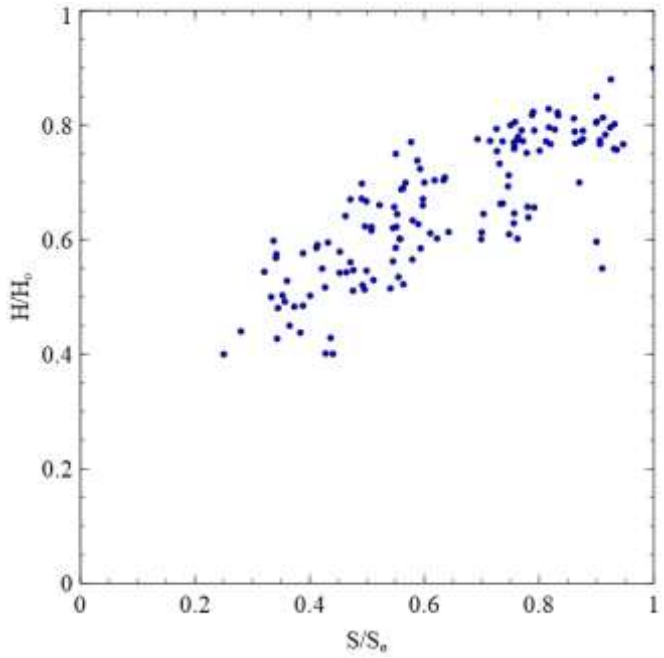

Fig. 1. Data quality control of clearness index and sunshine duration fraction.

Outliers were defined as data points that were outside of the envelope and were rejected before the data was used in the study. After the analysis, 0.276% of the data was rejected and deemed unsuitable. Similar studies including that of Nwokolo et al. [26] applied this technique on clearness index and sunshine duration fraction data from meteorological stations in Nigeria and observed a 0.34% data reduction in the sample data.

1.6 Development of Angstrom-Prescott Type Models

1.6.1 Computation of Regression Coefficients

The regression coefficient, a, in Eq. (6) indicates the fraction of extra-terrestrial radiation on a maximum overcast day, and the regression coefficient, b, represents the rate of increase of clearness index with respect to sunshine hours. Monthly and annual regression coefficients, a and b, were computed from the monthly values of clearness index, H/Ho, and sunshine duration fraction, S/So, by means of scatter plots.

Table 2. *Annual Angstrom-Prescott coefficients for selected stations.*

Station	Angstrom-Prescott coefficients		
	a	b	R^2
Beitbridge	0.29 77	0.4770	0.6394
Grand Reef	0.2765	0.5108	0.9030
Gweru	0.2252	0.6265	0.8849
Mt Darwin	0.3066	0.4807	0.7986
Nyanga	0.2362	0.6080	0.8601
Victoria Falls	0.2677	0.5912	0.8391

Notes. The regression coefficients, a and b, represent the y-intercept and the gradient of the regression equation respectively and R^2 represents the coefficient determination for each station.

The monthly regression coefficients developed for selected locations are shown in Table 2 which were developed from monthly clearness index and sunshine duration fractions from each station. For the annual A-P coefficients linear regression lines were plotted for each station which expressed the regression coefficients, a and b, as the linear y-intercept and gradient of each line respectively.

$$\frac{H}{H_o} = a + b\frac{S}{S_o} \qquad (6)$$

The variations of the Angstrom-Prescott type regression coefficients, *a* and *b*, with geographic variables like elevation,

latitude and longitude were computed as shown in **Error! Reference source not found.** in order to determine and illustrate the effect of these variables on the coefficients.

1.6.2 Generation of Estimated Solar Radiation Values

The developed monthly regression coefficients, a and b, together with the sunshine duration measurements, *S*, monthly extra-terrestrial solar radiation, H_o, and maximum sunshine duration values, S_o, from each station, were used to estimate monthly global solar radiation, H_e, using the Angstrom-Prescott type models for each station. For the nineteen stations with both historical solar radiation data and current calibrated solar radiation data, both sets of data were combined to generate estimated values of, *H*, for the period of 1971 to 2000 (historical) and 2006 to 2020 (current). The remaining ten stations without ground measured historical solar radiation data, only the calibrated solar radiation data from 2006 to 2020 was utilised to generate estimated solar radiation values.

1.7 Model Validation and Statistical Analysis

1.7.1 Model validation

To evaluate the model, estimated solar radiation values generated by the general model were compared with measured solar radiation values for each individual station. The estimated and measured values of global solar radiation, H_e and H_m, respectively from each station were compared using statistical analysis methods. The coefficients of Determination, R^2, obtained from the plots between measured and estimated solar radiation values were used to determine the relation between the two values. The relationship increases positively when the correlation coefficient increases from 0 to 1 [81,82].

1.7.2 Model performance analysis

Performance analysis of the models was done using the approaches which include the coefficient of determination (R^2), Mean Absolute Percentage Error (MAPE), Residual Mean Square Error (RMSE), Mean Absolute Error (MAE) and the Relative Standard Error (RSE) respectively shown by Eq. (7) – (11). The acceptable range for MAPE and RSE is between 0% and 10% and for RMSE and MAE is between 0 and 10 MJ/m^2 when comparing estimated and measured solar radiation values, and these statistical evaluation methods are the most commonly used to evaluate empirical models [26,61,64,69,83–85]. MAPE values less than 10% indicate a good precision model [16,86]. The closer the RMSE values are to zero the more accurate the model is and a value of RMSE equals zero is the ideal value [16,50,87].

$$R^2 = \frac{RSS}{TSS} \tag{7}$$

$$MAPE = \left| \left[\frac{\sum_{i=1}^{n} \left(\frac{H_{i,e} - H_{i,m}}{H_{i,m}} \right)}{n} \right] \times 100 \right| \tag{8}$$

$$RMSE = \sqrt{\frac{\sum_{i=1}^{n} \left(H_{i,e} - H_{i,m} \right)^2}{n}} \tag{9}$$

$$MAE = \frac{\sum_{i=1}^{n} \left| \left(H_{i,e} - H_{i,m} \right) \right|}{n} \tag{10}$$

$$RSE = \sqrt{\frac{\sum_{i=1}^{n} \left(\frac{H_{i,e} - H_{i,m}}{H_{i,m}} \right)^2}{n}} \tag{11}$$

Where, RSS is the residuals sum of squares and TSS is total sum of squares, *i*, is the, i^{th}, value and, *n*, is the total number of measured or estimated values.

2 Results and Discussions

2.1 Satellite data correction

Each satellite-based measurement was paired with a corresponding ground measurement for each month measured between the years 2006 to 2020. As a result a correction equation was generated relating ground-measured data, H_{grn}, to Satellite based data, H_{sat}, as shown by Eq. (12) and Fig 2.

$$H_{grn} = 3.7114 + 0.7568 H_{sat} \tag{12}$$

In Fig. 2 the coefficient of correlation r = 0.8209 (R^2 = 0.6738) shows a high positive relationship between, H_{grn}, and, H_{sat}, hence, r, was regarded a high enough coefficient of correlation to support the use of Eq. (12). The satellite-based solar radiation data is consistent in terms of measurement, hence the correction equation obtained from the mini-station was used to generate current ground-based values from corresponding satellite-based values for the other 29 meteorological stations.

2.2 Characterization of Meteorological Parameters

The averages of global solar radiation, *H*, extra-terrestrial solar radiation, H_o, sunshine duration, *S*, maximum sunshine duration, S_o, the clearness index, H/H_o, and fraction of sunshine duration, *S/So*, for selected stations are presented in Table 1. In Table 1, it can be seen that the, *H*, *S*, H/H_o, and, S/S_o, differ for each station and these variabilities can be attributed to the latitude, longitude and altitude of each location-based station. In Table 1, it can be observed that, H/H_o and S/S_o, reduce in magnitude as the longitude increase from the east to the west of Zimbabwe. According to the Koppen-Geiger classifications the western part of the country is semi-arid hence experiences much more solar radiation with increased sunshine hours and these variables reduce towards the eastern part of the country in the eastern highlands with subtropical highland climate. This then implies that locations based in the western part of Zimbabwe receive increased solar radiation than locations close or within the

eastern highlands due to the atmospheric differences between the two regions.

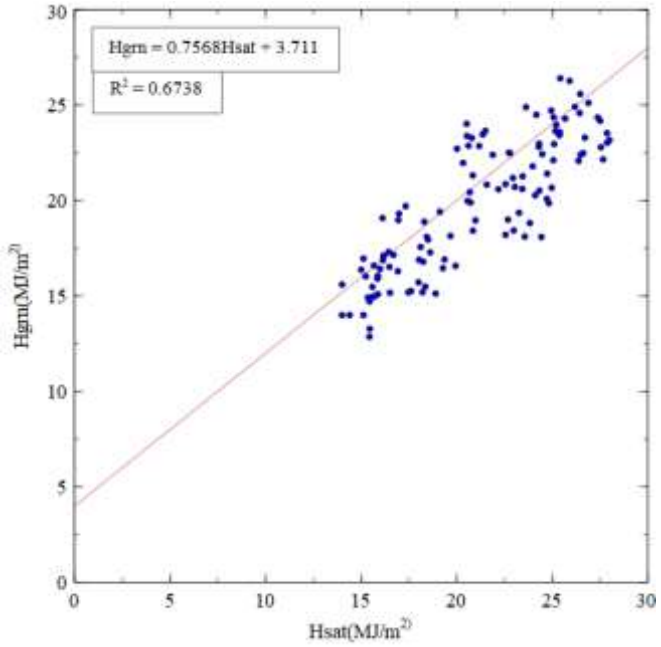

Fig. 2. Ground and satellite measured data correlation. University of Zimbabwe (2006-2020).

According to the World Meteorological Organization [88], the fraction of sunshine duration (S/S_o) classifications are as follows: Cloudy sky $0 \leq \frac{S}{S_o} < 0.3$, Scattered clouds $0.3 \leq \frac{S}{S_o} < 0.7$ and Clear sky $0.7 \leq \frac{S}{S_o} < 1.0$.

The locations under study show a mixture of scattered clouds and clear sky characteristics. Seventeen of the stations indicated scattered clouds predominance, whilst twelve of the stations indicated clear sky predominance, which are mainly located in the semi-arid regions of the country. The least sunshine duration fraction was 0.1588 at Mukandi Meteorological Station located in the eastern highlands with subtropical highland climate, whilst the highest sunshine duration fraction was 0.7494 at Victoria Falls Meteorological Station located in the north-west part of the country with semi-arid climatic conditions. WMO (2018) classifies the monthly clearness index, H/H_o, into three meteorological classifications as follows: Very cloudy weather ($H/H_o \leq 0.4$), partially covered weather ($0.4 \leq H/H_o \leq 0.7$) and Clear weather ($H/H_o \geq 0.7$). The generalised datasets shown in Table 1 indicated that for all the stations under study the predominant meteorological condition is partly cloudy with average clearness index between 0.5 and 0.7. The lowest clearness index was 0.3352 at Mukandi Meteorological Station and the highest was recorded at Victoria Falls Meteorological Station as 0.7107.

2.3 Relationships between H/Ho and S/S_o

To generate the Angstrom-Prescott type regression coefficients, *a* and *b*, for each station plots between the clearness indexes, H/H_o, and the sunshine duration fractions, were generated as represented in figure 3. In Fig. 3(a) to Fig. 3(d), it can be observed that, *H*, and, H/H_o, increase with increasing, *S*, and S/S_o, as expected for each station. Solar radiation received increases with increase in sunshine duration and the quantities can be attributed to the type of Koppen-Geiger climate classification of each location station [26]. The highest correlation between the clearness index and the sunshine duration fraction was 0.9030 as shown in Table 2 with 80% of the stations having R^2, greater than 0.6. The lowest, R^2, is 0.3387 for Buffalo Range station in Chiredzi which can be considered a weak correlation, as it is evident by dispersed data showing a weak relationship between, H/H_o, and S/S_o, as shown in Fig 3(c).

Table 3. *Monthly Angstrom-Prescott type regression coefficient, a, for selected locations.*

Station	Month											
	Jan	Feb	Mar	Apr	May	Jun	Jul	Aug	Sep	Oct	Nov	Dec
Beitbridge	0.31	0.29	0.27	0.32	0.33	0.42	0.59	0.32	0.38	0.26	0.31	0.33
Grand Reef	0.32	0.26	0.35	0.33	0.38	0.24	0.28	0.40	0.24	0.23	0.49	0.28
Gweru	0.32	0.29	0.24	0.20	0.27	0.25	0.39	0.42	0.29	0.21	0.28	0.29
Kutsaga	0.33	0.33	0.44	0.44	0.28	0.55	0.66	0.48	0.31	0.61	0.62	0.48
Mt Darwin	0.31	0.32	0.32	0.35	0.42	0.37	0.44	0.40	0.33	0.33	0.30	0.32
Nyanga	0.31	0.28	0.30	0.34	0.39	0.37	0.29	0.34	0.25	0.23	0.29	0.29
Vic. Falls	0.29	0.29	0.31	0.10	0.08	0.06	0.16	0.52	0.31	0.30	0.33	0.30

Table 4. *Monthly Angstrom-Prescott type regression coefficient, b, for selected locations.*

Stations	Month											
	Jan	Feb	Mar	Apr	May	Jun	Jul	Aug	Sep	Oct	Nov	Dec
Beitbridge	0.45	0.47	0.53	0.47	0.46	0.31	0.10	0.46	0.36	0.53	0.45	0.42
Grand Reef	0.43	0.52	0.40	0.46	0.41	0.57	0.53	0.37	0.54	0.54	0.13	0.50
Gweru	0.43	0.50	0.60	0.66	0.60	0.63	0.45	0.40	0.52	0.61	0.50	0.50
Kutsaga	0.37	0.35	0.22	0.27	0.52	0.20	0.07	0.27	0.43	0.02	0.12	0.04
Mt Darwin	0.47	0.44	0.47	0.45	0.38	0.45	0.34	0.37	0.41	0.39	0.44	0.45
Nyanga	0.44	0.49	0.49	0.47	0.44	0.49	0.58	0.49	0.56	0.56	0.46	0.48
Vic. Falls	0.55	0.56	0.54	0.81	0.83	0.95	0.72	1.45	0.51	0.52	0.49	0.55

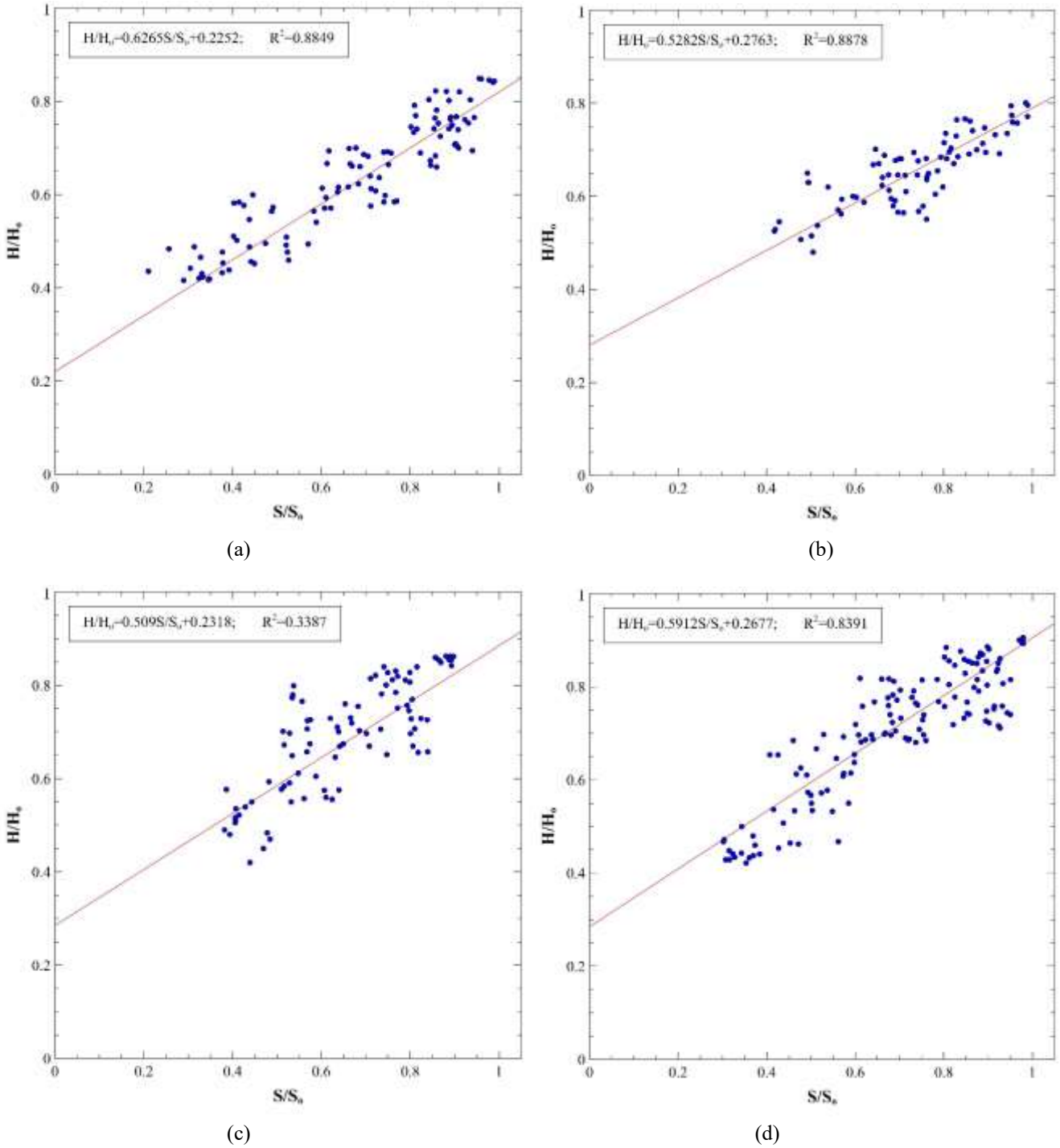

Fig. 3. Correlation plot between H/Ho and S/So for (a) Gweru, (b) Grand Reef, (c) Buffalo Range and (d) Victoria Falls.

Table 5. *The variation of the annual A-P coefficients with meteorological and climatic variables.*

Station	Latitude (º)	Longitude (º)	Elevation (m)	S/So	H/Ho	a	b
Beitbridge	22.22	29 .99	457.00	0.7135	0.6380	0.2977	0.4770
Grand Reef	18.98	32.45	1019.00	0.6878	0.6529	0.2763	0.5282
Gweru	19.45	29 .85	1429 .00	0.7001	0.6638	0.2252	0.6265
Kutsaga	17.92	31.13	1480.00	0.6996	0.6152	0.2855	0.4707
Mt Darwin	16.78	31.58	953.00	0.6900	0.6383	0.3066	0.4807
Nyanga	18.22	32.75	1679.00	0.6458	0.6288	0.2362	0.6080
Victoria Falls	17.93	25.85	1062.00	0.7494	0.7107	0.2677	0.5912

***Note. H/H_o*, is the clearness index, *S/S_o*, is the sunshine duration fraction, *a* and *b*, are the Angstrom-Prescott regression coefficients.**

2.4 Angstrom-Prescott Regression Coefficients

In both Table 2, 3 and 4 it can be observed that both, a and b, are higher in the winter months of May to August and are lower in the summer and wet months of October to March. This can be attributed to the clear sky conditions during the winter and cloudy skies experienced in the summer in Zimbabwe. The plots in Fig. *3*, as well as Tables 2, 3 and 4 show the annual Angstrom-Prescott type regression coefficients, a and b, which are the gradient and y-intercepts respectively for all the stations under study. The correlation coefficient, a, ranged from 0.2252 at Gweru Meteorological Station to 0.3976 at Chisengu Meteorological Station and the correlation coefficient, b, ranged from 0.3218 at Banket Meteorological Station to 0.6265 at Gweru Meteorological Station.

Table 5, shows the variations of regression coefficients, *a* and *b*, with respect to latitude, longitude, elevation, S/S_o and H/H_o. It can be seen that both the regression coefficient, *a* and *b*, do not possess a salient relationship with the variables particularly latitude and elevation. The above trends were also observed in other similar studies [48,50,89,90], where the outcomes showed that neither *a* nor *b*, varied with latitude and altitude in any systematic manner. This can be attributed to the lack of distribution between the stations across the whole Zimbabwe as the bulk of the stations are located in the North-Western and Western part of the country.

However there is a slight effect on both, a and b, with respect to the longitude. The value of, *a*, tends to reduce as the longitude increases, whilst the value of, *b*, increases with increase in longitude as shown in Table 5. This implies that the values of, *a*, are higher in the western parts of the country as seen in the stations like Victoria Falls (a = 0.2677, b = 0.5912) and Binga (a = 0.3222, b = 0.4795) and lower in the eastern parts in stations like Nyanga (a = 0.2362, b = 0.6080) and Mukandi (a = 0.2100, b = 0.5340) and vice versa for the values of *b*. Therefore it can be assumed that the values of a and b at a location are dominantly affected by the climatic condition of the area. Particularly in Zimbabwe it can be observed that areas with semi-arid climates have high values of *a*, than those areas with a subtropical climate and vice versa for the values of *b*. [26] deduced similar conclusions from a similar research, whereby the stations that are within the hot desert and the warm semi-arid climates of Nigeria showed higher coefficients of *a*, between 0.350 and 0.469 compared to the station that are within the tropical savannah and the tropical rainforest climates with *a*, values between 0.212 and 0.268. [26] also obtained values of the AP coefficient *b*, which increased from stations within the hot (arid) desert climate to those in the tropical rainforest climate.

The Angstrom-Prescott type models for various areas in Zimbabwe based on individual station are shown in table 6. It can be observed that a few stations like Banket (a = 0.3356, b = 0.3218), Chisengu (a = 0.3306, b = 0.3333) and Triangle (a = 0.3223, b = 0.3287) exhibited values of a and b, that are off trend with a very small difference between the a and b, values. This can be attributed to the use of only satellite-based solar radiation data for these stations which had slightly higher values than ground-measured values used in other stations. The coefficient *a*, from literature indicates the proportion of H_o, received on the surface on a very cloudy day when S/S_o = 0, whilst $a + b$, indicate the proportion of H_o, on a clear sky day when $S/S_o = 1$ [26]. This indicates that the higher intensity of *H*, received the greater the value of *a*, and the less the value of *b*. The variations mentioned above were also obtained by [27,64] in similar researches where both satellite and ground data were used interchangeably and the implication of these findings in both cases reduced the predicting power of the models slightly. In the case of [27] the predicting power of the models based on satellite data was reduced by 1.48%.

The Angstrom-Prescott type models obtained in table 5 show similarities in the regression coefficients of a and b, for stations in close proximity like MSD Belvedere with a = 0.2886 and b = 0.4635 and Kutsaga with a = 0.2855 and b = 0.4707 all located in Harare. The above regression coefficients for the stations based in Harare also showed similarities with the coefficients obtained by [51] for Harare with a = 0.282 and b = 0.460. Hove and Göttsche [63] also obtained similar coefficients for Gokwe and West Nicholson as (a = 0.36, b = 0.47) and (a = 0.29 , b = 0.49) respectively as shown in Table 5.

2.5 Estimated Solar Radiation Values

The models in Table 6 were used to estimate monthly solar radiation values H_e, for each station and the values were compared to the monthly measured and extra-terrestrial solar radiation from individual stations H_{grn} and H_o respectively. Monthly H_e and H_{grn}, were plotted and a selected plot for Nyanga is shown in Fig. 4.

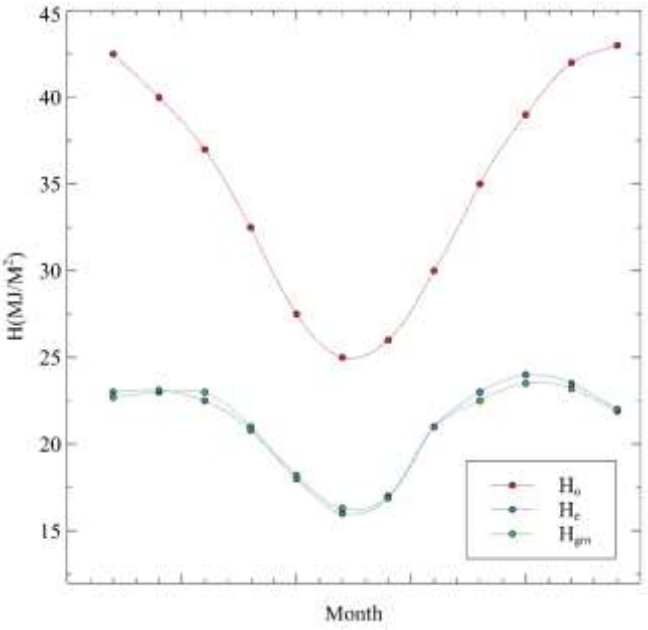

Fig. 4. Comparison between H_e, H_{grn} and H_o for Nyanga Station.

The extra-terrestrial solar radiation H_o, maintained a similar trend in all the stations as shown in Fig. 4 with a steep U-shaped plot. H_o ranged between 23MJ/m^2 and 44 MJ/m^2, with the lowest values observed in the months of June, July and August (winter season), and the highest in the months of October, November, December and January (summer season). In Fig. 4, it can be seen that both the estimated and measured monthly solar radiation values follow the same trend as the monthly Extra-terrestrial solar radiation values but with a gentle U-shaped slope which drops from the month of March to July and rises from August to October and drops slightly from November to December. In Zimbabwe the months of June and July are the coldest months, with August being windy and while the month of October is the hottest. The months of November, December and March are the wettest months and all these variations related to altitude [65]. H_e and H_{grn}, had values ranging between 12 MJ/m^2 and 27 MJ/m^2, with the lowest values observed in the months of June and July, and the highest in the month of October.

The slight drop in magnitude of the measured and estimated solar radiation values from the months of October to December can be attributed to effect of rain, with the rain season beginning in late October or early November [65]. Observing the values of both extra-terrestrial and measured global horizontal solar irradiation it can be concluded that just above 50 % of the extra-terrestrial solar irradiation from the sun is received on the ground and this can be attributed mostly to the effect of the atmosphere. The trends observed in Fig 4. are similar to the trends observed in other studies in countries surrounding Zimbabwe [81,90–92] in Mozambique, South Africa, South Africa and Malawi respectively. The estimated values H_e, show very small variations from the measured values H_{grn}, in most of the stations, except for Buffalo Range which exhibit slightly higher variations.

The estimated values H_e, for the general model were compared to ground measured values, H_{grn}, and extra-terrestrial H_o, solar radiation values from individual stations to assess the deviation from the measured values. It was noted that the general model estimated values, H_e, maintained the same trend as H_{grn}, for all the stations. Slight deviations between, H_e and H_{grn}, can however be observed in a few stations such as Banket, Chisumbanje, Chivhu, Gokwe, Kariba and Triangle. These slight deviations are attributed to the input solar radiation data used from these stations, which was ground corresponding values based on satellite measurements only.

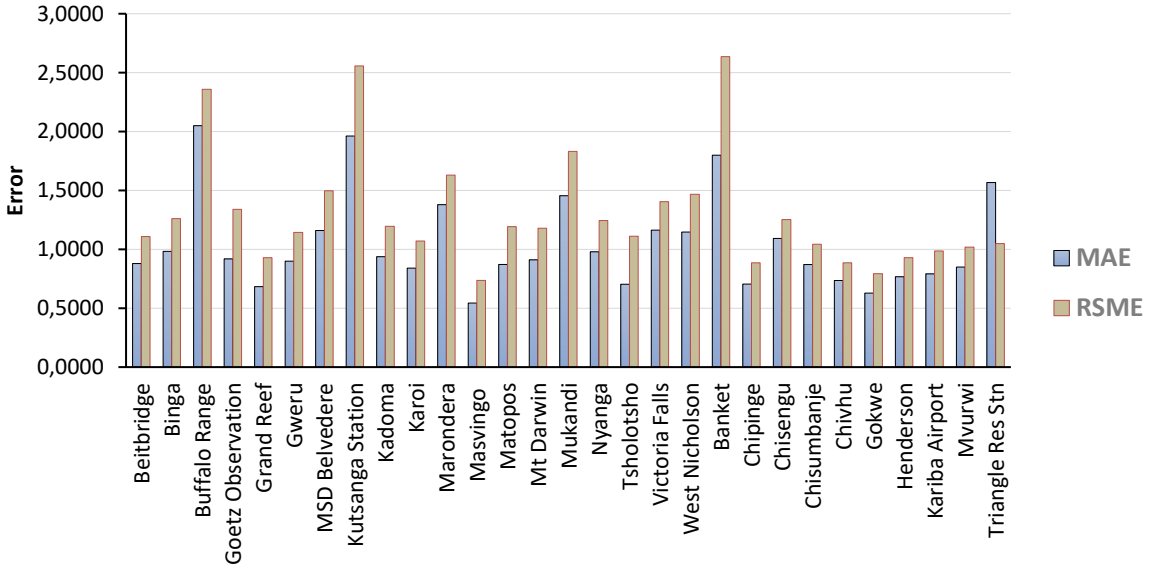

Fig. 5. The Mean Absolute Error and Root Square Mean Error for each station.

Table 6. *Angstrom-Prescott Type Models for each station.*

Station	Model	Station	Model
Beitbridge	$\frac{H}{H_o} = 0.2977 + 0.4770\frac{S}{S_0}$	Nyanga	$\frac{H}{H_o} = 0.2362 + 0.6080\frac{S}{S_0}$
Binga	$\frac{H}{H_o} = 0.3222 + 0.4795\frac{S}{S_0}$	Tsholotsho	$\frac{H}{H_o} = 0.2389 + 0.5307\frac{S}{S_0}$
Buffalo Range	$\frac{H}{H_o} = 0.2763 + 0.5090\frac{S}{S_0}$	Victoria Falls	$\frac{H}{H_o} = 0.2677 + 0.5912\frac{S}{S_0}$
Goetz Obs	$\frac{H}{H_o} = 0.2808 + 0.4670\frac{S}{S_0}$	West Nicholson	$\frac{H}{H_o} = 0.2931 + 0.5003\frac{S}{S_0}$
Gweru	$\frac{H}{H_o} = 0.2252 + 0.6265\frac{S}{S_0}$	Chisengu	$\frac{H}{H_o} = 0.3306 + 0.3333\frac{S}{S_0}$
MSD Belvedere	$\frac{H}{H_o} = 0.2886 + 0.4635\frac{S}{S_0}$	Chipinge	$\frac{H}{H_o} = 0.3976 + 0.4866\frac{S}{S_0}$
Kutsaga	$\frac{H}{H_o} = 0.2855 + 0.4707\frac{S}{S_0}$	Chisumbanje	$\frac{H}{H_o} = 0.2559 + 0.4206\frac{S}{S_0}$
Kadoma	$\frac{H}{H_o} = 0.2785 + 0.5099\frac{S}{S_0}$	Chivhu	$\frac{H}{H_o} = 0.3479 + 0.5108\frac{S}{S_0}$
Karoi	$\frac{H}{H_o} = 0.3041 + 0.5469\frac{S}{S_0}$	Gokwe	$\frac{H}{H_o} = 0.3634 + 0.4864\frac{S}{S_0}$
Marondera	$\frac{H}{H_o} = 0.2658 + 0.5605\frac{S}{S_0}$	Henderson	$\frac{H}{H_o} = 0.3723 + 0.4923\frac{S}{S_0}$
Masvingo	$\frac{H}{H_o} = 0.2743 + 0.5054\frac{S}{S_0}$	Kariba Airport	$\frac{H}{H_o} = 0.3147 + 0.3244\frac{S}{S_0}$
Matopos	$\frac{H}{H_o} = 0.2562 + 0.5298\frac{S}{S_0}$	Mvurwi	$\frac{H}{H_o} = 0.3871 + 0.4667\frac{S}{S_0}$
Mt Darwin	$\frac{H}{H_o} = 0.3066 + 0.4807\frac{S}{S_0}$	Triangle	$\frac{H}{H_o} = 0.3223 + 0.3287\frac{S}{S_0}$
Mukandi	$\frac{H}{H_o} = 0.3100 + 0.5340\frac{S}{S_0}$	Harare	$\frac{H}{H_o} = 0.2820 + 0.4600\frac{S}{S_0}$

Note. The correlation coefficients, a and b, are the gradient and y-intercepts respectively.

2.6 Statistical Evaluation of the Models

The estimated and measured values of global solar radiation H_e and H_{grn}, respectively from each station were compared using statistical analysis methods in order to evaluate each model's potential to predict solar irradiation. The analytical methods used to evaluate the models were the mean absolute percentage error (MAPE), the root mean square error (RMSE), the mean absolute error (MAE) and the relative standard error (RSE) and the results are shown in Table 7.

The Mean Absolute Error values for each model range from 0.5438 MJ/m^2 to 2.2845 MJ/m^2. The small values of Mean Absolute Errors between the measured and estimated solar radiation values indicate very good long-term prediction capabilities of the models. The Mean Absolute Percentage Errors indicate a range between 2.5642 % and 10.3343 %. It was noted that only Buffalo Range Station out of the 29 stations had a Mean Absolute Percentage Error greater than 10 % and this can be attributed to the low correlation coefficients value between the clearness index and the sunshine duration fraction expressed by the station. The low correlation coefficient was due to inaccurate sunshine duration data for the station obtained from MSD, which was mainly due to faulty measuring instruments. The rest of the stations indicated Mean Absolute Percentage Errors between estimated and measured solar radiation values to be lower

than 10%, hence showing very high predicting abilities as observed in other studies [16,81,86].

Table 7. *Results of the Statistical Evaluation of the Angstrom-Prescott Type Models.*

Station	R^2	MAE (MJ/m^2)	MAPE (%)	RSME (MJ/m^2)	RSE (%)
Beitbridge	0.9154	0.8792	4.1974	1.1095	0.0528
Grand Reef	0.9329	0.6830	3.1807	0.9280	0.0425
Gweru	0.8793	0.8994	3.9684	1.1446	0.0501
Mt Darwin	0.8707	0.9106	4.229 0	1.1787	0.0549
Nyanga	0.8782	0.9789	4.6161	1.2444	0.0582
Victoria Falls	0.7612	1.1629	4.8627	1.4034	0.0583

The Relative Standard Error for the models was found to be between 0.0346 % and 0.1537% showing very low values of the standard error relative to the estimated values, hence indicating high degrees of accuracy of estimation correlations in the models similar to values of RSE found in other studies by [25,83]. The Relative Mean Square Errors for the models ranged from 0.7360 MJ/m^2 to 2.9454 MJ/m^2 and these values are within the recommended range for excellent solar predicting models from other similar studies [50,87], hence indicating good short-term predicting capabilities for all the models. As shown in Fig. 5., Masvingo Station exhibited very low values of MAE, MPE, RSE and RMSE which can be attributed to the high correlation coefficient of r = 0.9531 between the estimated and measured solar radiation values. Triangle station in Chiredzi exhibited the highest values of MAE, MPE, RSE, RMSE and a low coefficient of determination R^2 = 0.6062 between the estimated and measured values of solar radiation.

The results of the statistical analysis for the general model which were compared to the results for the individual station-based models show very slight changes for MAE, MAPE, RMSE and RSE in most of the stations. This confirms the high predicting capabilities of the general model. Significant changes can be observed under MAPE statistical analysis particularly for the stations with satellite-based solar radiation data, but however the changes still remained within the required limit of 0% < MAPE < 10%.

3 CONCLUSION

The main aim of this study was to develop a general Angstrom-Prescott type model for predicting solar irradiation in Zimbabwe. In the process of predicting solar irradiation using empirical coefficients, sunshine duration was deemed to have the greatest impact on the amount of solar radiation received on a horizontal surface.

The following notable results were reported.

- The highest correlation between the clearness index and the sunshine duration fraction was 0.9030 with 80% of the coefficients of determination above 0.6.
- The results of the study showed no systematic trend between the regression coefficients with both latitude and elevation, however the value of, *a*, decreased as the longitude increases, whilst the value of, *b*, increased with increase in longitude, hence the values of, *a*, were higher in the western parts of the country and lower in the eastern parts and vice versa for the values of, *b,* and these results agreed with other results from similar researches.
- The MAE values for the models ranged from 0.5438 MJ/m^2 to 2.2845 MJ/m^2. The MAPE indicated a range between 2.5642 % and 10.334 % with only Buffalo Range Station having a MAPE greater than 10 % which was caused by a faulty sunshine recorder. The rest of the stations indicated MAPE values lower than 10 %, hence showing very high predicting abilities.
- The values of the regression coefficients, a and b, at a location are dominantly affected by the climatic condition of the area and that the more specific the coefficients are to a location the more accurate they become.
- Also the general model developed in this study is considered to have good solar prediction abilities as proven by statistical results that are within the recommended range.
- The developed models can provide estimated solar irradiation data that is currently not available in the meteorological stations in Zimbabwe, hence filling the gap in terms of solar radiation data availability.

4 NOMENCLATURE

A-P	Angstrom-Prescott	NASA	National aeronautics and space administration
DAS	Data assimilation system		
GHG	Greenhouse gas	RMSE	Root mean square error
H	Global Horizontal Irradiation (MJ/m^2)	RH	Relative Humidity
H_e	Estimated solar radiation (MJ/m^2)	r	Coefficient of Correlation
H_{grn}	Ground measured solar radiation (MJ/m^2)	R^2	Coefficient of Determination
H_{sat}	Satellite measured solar radiation (MJ/m^2)	S	Actual sunshine duration (Hours)
H_o	Extra-terrestrial solar radiation (MJ/m^2)	S_o	Extra-terrestrial sunshine duration (Hours)
MAE	Mean abstract error	UNFCCC	United nations framework convention on climate change
MAPE	Mean abstract percentage error		
MERRA	Modern-era retrospective analysis for research and applications	XGBoost	Extreme gradient boosting
		φ	Latitude
MSD	Meteorological service department	δ	Standard deviation
n	Day number		

5 REFERENCES

[1] Syed, A., Raza, T., Bhatti, T.T., and Eash, N.S. (2022) Climate Impacts on the agricultural sector of Pakistan: Risks and solutions. *Environmental Challenges*, **6**, 100433.

[2] Patel, R.V., Yadav, A., and Winczek, J.A. (2021) Experimental Investigation and Mathematical Modelling of Heat Transfer Coefficient in Double Slope Solar Still. *SV-JME*, **67** (7–8), 369–379.

[3] Leal Filho, W., Wall, T., Rui Mucova, S.A., Nagy, G.J., Balogun, A.-L., Luetz, J.M., Ng, A.W., Kovaleva, M., Safiul Azam, F.M., Alves, F., Guevara, Z., Matandirotya, N.R., Skouloudis, A., Tzachor, A., Malakar, K., and Gandhi, O. (2022) Deploying artificial intelligence for climate change adaptation. *Technological Forecasting and Social Change*, **180**, 121662.

[4] Taghavipour, A., and Alipour, A. (2021) HIL Evaluation of a Novel Real-time Energy Management System for an HEV with a Continuously Variable Transmission. *SV-JME*, **67** (4), 142–152.

[5] Hargrove, A., Qandeel, M., and Sommer, J.M. (2019) Global governance for climate justice: A cross-national analysis of CO2 emissions. *Global Transitions*, **1**, 190–199.

[6] New, M., Liverman, D., Schroder, H., and Anderson, K. (2011) Four degrees and beyond: the potential for a global temperature increase of four degrees and its implications. *Phil. Trans. R. Soc. A.*, **369** (1934), 6–19.

[7] Bayrakçı, H.C., Demircan, C., and Keçebaş, A. (2018) The development of empirical models for estimating global solar radiation on horizontal surface: A case study. *Renewable and Sustainable Energy Reviews*, **81**, 2771–2782.

[8] Holechek, J.L., Geli, H.M.E., Sawalhah, M.N., and Valdez, R. (2022) A Global Assessment: Can Renewable Energy Replace Fossil Fuels by 2050? *Sustainability*, **14** (8), 4792.

[9] Tierney, S., and Bird, L. (2020) Setting the Record Straight About Renewable Energy.

[10] Felix, P.G., Rajagopal, V., and Kumaresan, K. (2021) Applicability of MCDM Algorithms for the Selection of Phase Change Materials for Thermal Energy Storage Heat Exchangers. *SV-JME*, (11), 611–622.

[11] Kittusamy, R.K., Rajagopal, V., and Felix, P.G. (2022) Preparation and Thermal Characterization of Nanographene- Enhanced Fatty Acid-Based Solid-Liquid Organic Phase Change Material Composites for Thermal Energy Storage. *sv-jme*, **68** (7–8), 461–470.

[12] Bouchouicha, K., Hassan, M.A., Bailek, N., and Aoun, N. (2019) Estimating the global solar irradiation and optimizing the error estimates under Algerian desert climate. *Renewable Energy*, **139**, 844–858.

[13] Ballantyne, E.E.F., Nunez Munoz, M., and Stone, D.A. (2022) Development and evaluation of empirical models for the estimation of hourly horizontal diffuse solar irradiance in the United Kingdom. *Energy*, **241**, 122820.

[14] Mohamad, N.B., Lai, A.-C., and Lim, B.-H. (2022) A case study in the tropical region to evaluate univariate imputation methods for solar irradiance data with different weather types. *Sustainable Energy Technologies and Assessments*, **50**, 101764.

[15] AlKandari, M., and Ahmad, I. (2020) Solar power generation forecasting using ensemble approach based on deep learning and statistical methods. *Applied Computing and Informatics*, **ahead-of-print** (ahead-of-print).

[16] Djoman, M.A., Fassinou, W.F., and Memeledje, A. (2021) Calibration of Ångström-Prescott Coefficients to Estimate Global Solar Radiation in Côte d'Ivoire. *European Scientific Journal, ESJ*, **17** (37), 24–24.

[17] Jebli, I., Belouadha, F.-Z., Kabbaj, M.I., and Tilioua, A. (2021) Prediction of solar energy guided by pearson correlation using machine learning. *Energy*, **224**, 120109.

[18] Wang, Y., Feng, B., Hua, Q.-S., and Sun, L. (2021) Short-Term Solar Power Forecasting: A Combined Long Short-Term Memory and Gaussian Process Regression Method. *Sustainability*, **13** (7), 3665.

[19] Ye, H., Yang, B., Han, Y., and Chen, N. (2022) State-Of-The-Art Solar Energy Forecasting Approaches: Critical Potentials and Challenges. *Frontiers in Energy Research*, **10**.

[20] Chukwujindu Nwokolo, S., Ogbulezie, J.C., and Umunnakwe Obiwulu, A. (2022) Impacts of climate change and meteo-solar parameters on photosynthetically active radiation prediction using hybrid machine learning with Physics-based models. *Advances in Space Research*, **70** (11), 3614–3637.

[21] Nwokolo, S.C., Obiwulu, A.U., Ogbulezie, J.C., and Amadi, S.O. (2022) Hybridization of statistical machine learning and numerical models for improving beam, diffuse and global solar radiation prediction. *Cleaner Engineering and Technology*, **9**, 100529.

[22] Obiwulu, A.U., Erusiafe, N., Olopade, M.A., and Nwokolo, S.C. (2022) Modeling and estimation of the optimal tilt angle, maximum incident solar radiation, and global radiation index of the photovoltaic system. *Heliyon*, **8** (6), e09598.

[23] Keshtegar, B., Bouchouicha, K., Bailek, N., Hassan, M.A., Kolahchi, R., and Despotovic, M. (2022) Solar irradiance short-term prediction under meteorological uncertainties: survey hybrid artificial intelligent basis music-inspired optimization models. *Eur. Phys. J. Plus*, **137** (3), 362.

[24] Arslanoglu, N. (2022) Development of empirical models for estimation diffuse solar radiation exergy in Turkey. *IJEX*, **37** (1), 24.

[25] Lare, Y., Sambiani, K., Amega, K., and Kabe, M. (2021) Modeling of the Global Daily Horizontal Solar Radiation Data over Togo. *Energy and Power Engineering*, **13** (12), 403–412.

[26] Nwokolo, S.C., Amadi, S.O., Obiwulu, A.U., Ogbulezie, J.C., and Eyibio, E.E. (2022) Prediction of global solar radiation potential for sustainable and cleaner energy generation using improved Angstrom-Prescott and Gumbel probabilistic models. *Cleaner Engineering and Technology*, **6**, 100416.
[27] Oyewola, O.M., Patchali, T.E., Ajide, O.O., Singh, S., and Matthew, O.J. (2022) Global solar radiation predictions in Fiji Islands based on empirical models. *Alexandria Engineering Journal*, **61** (11), 8555–8571.
[28] Caycedo Villalobos, L.A., Cortázar Forero, R.A., Cano Perdomo, P.M., and González Veloza, J.J.F. (2021) Solar Radiation Prediction Using Machine Learning Techniques, in *Applied Informatics*, vol. 1455, Springer International Publishing, Cham, pp. 68–81.
[29] Deo, R.C., and Şahin, M. (2017) Forecasting long-term global solar radiation with an ANN algorithm coupled with satellite-derived (MODIS) land surface temperature (LST) for regional locations in Queensland. *Renewable and Sustainable Energy Reviews*, **72**, 828–848.
[30] Khatib, T., Mohamed, A., Sopian, K., and Mahmoud, M. (2012) Solar Energy Prediction for Malaysia Using Artificial Neural Networks. *International Journal of Photoenergy*, **2012**, 1–16.
[31] Kim, Y.S., Joo, H.Y., Kim, J.W., Jeong, S.Y., and Moon, J.H. (2021) Use of a Big Data Analysis in Regression of Solar Power Generation on Meteorological Variables for a Korean Solar Power Plant. *Applied Sciences*, **11** (4), 1776.
[32] Kor, H. (2021) Global solar radiation prediction model with random forest algorithm. *Therm sci*, **25** (Spec. issue 1), 31–39.
[33] Zhang, X., Zhang, M., Cui, Y., and He, Y. (2022) Estimation of Daily Ground-Received Global Solar Radiation Using Air Pollutant Data. *Frontiers in Public Health*, **10**.
[34] Sabbagh, J.A., Sayigh, A.A.M., and El-Salam, E.M.A. (1977) Estimation of the total solar radiation from meteorological data. *Solar Energy*, **19** (3), 307–311.
[35] Kasten, F., and Czeplak, G. (1980) Solar and terrestrial radiation dependent on the amount and type of cloud. *Solar Energy*, **24** (2), 177–189.
[36] Samuel Chukwujindu, N. (2017) A comprehensive review of empirical models for estimating global solar radiation in Africa. *Renewable and Sustainable Energy Reviews*, **78**, 955–995.
[37] Nwokolo, S.C., and Ogbulezie, J.C. (2018) A quantitative review and classification of empirical models for predicting global solar radiation in West Africa. *Beni-Suef University Journal of Basic and Applied Sciences*, **7** (4), 367–396.
[38] Bautista, G.M.R., and Chacón, C.A.C. (2021) Ångström-Prescott Models of Solar radiation over Earth surface. *J. Phys.: Conf. Ser.*, **2135** (1), 012005.
[39] Bristow, K.L., and Campbell, G.S. (1984) On the relationship between incoming solar radiation and daily maximum and minimum temperature. *Agricultural and Forest Meteorology*, **31** (2), 159–166.
[40] Donatelli, M., and Campbell, G.S. (1998) A simple model to estimate global solar radiation. *Proceedings of the 5th European society of agronomy congress, Nitra, Slovak Republic*, **2**, 133–134.
[41] Nwokolo, S., and Ogbulezie, J. (2017) A single hybrid parameter-based model for calibrating hargreaves-samani coefficient in Nigeria. *International Journal of Physical Research*, **5** (2), 49–59.
[42] Woldegiyorgis, T.A., Admasu, A., Benti, N.E., and Asfaw, A.A. (2022) A Comparative Evaluation of Artificial Neural Network and Sunshine Based models in prediction of Daily Global Solar Radiation of Lalibela, Ethiopia. *Cogent Engineering*, **9** (1), 1996871.
[43] Glover, J., and McCulloch, J.S.G. (1958) The empirical relation between solar radiation and hours of bright sunshine in the high-altitude tropics. *Quarterly Journal of the Royal Meteorological Society*, **84** (359), 56–60.
[44] Page, J.K. (1961) The estimation of monthly mean values of daily total short wave radiation on vertical and inclined surfaces from sunshine records for latitudes 40N-40S by /.
[45] Abramczyk, J. (2022) Parametric building forms rationalizing the incident direct solar irradiation. *Building and Environment*, **215**, 108963.
[46] Sankarayogi, P., Annareddy, R.R., Awasthi, A., Gugamsetty, B., Pulla, S.N., and Yadiki, N.A. (2022) Estimation of Monthly Mean Global Solar Radiation Over Semi-arid Region, Kadapa Using Meteorological Parameter.
[47] Bahel, V., Bakhsh, H., and Srinivasan, R. (1987) A correlation for estimation of global solar radiation. *Energy*, **12** (2), 131–135.
[48] Dehkordi, S.N., Bakhtiari, B., Qaderi, K., and Ahmadi, M.M. (2022) Calibration and validation of the Angstrom–Prescott model in solar radiation estimation using optimization algorithms. *Sci Rep*, **12** (1), 4855.
[49] Mostafazadeh, S., Behmanesh, J., and Rezaverdinejad, V. (2022) Evaluating the effect of the atmospheric pollutants on the received solar radiation by ground surface using Angstrom-Prescott model (Case study: Urmia and Tabriz). *Water and Soil Science*, **32** (1), 15–26.
[50] Mejia, J.R.R., Prieto, A.W., Chávez, A.V., Varela, R.V., López Monteagudo, F.E., and Rivas, C.R. (2022) Estimation of solar radiation in Northwest Mexico based on the Angstrom model and polynomial regression. *Ingeniería Energética*, **43** (1), 35–47.
[51] Lewis, G. (1983) Estimates of irradiance over Zimbabwe. *Solar Energy*, **31** (6), 609–612.
[52] Swartman, R.K., and Ogunlade, O. (1967) Solar radiation estimates from common parameters. *Solar Energy*, **11** (3), 170–172.
[53] Chagwedera, S.M., and Sendezera, E.J. (1991) Prediction of global solar radiation at two locations in Zimbabwe: a comparative analysis of three

Ångstrom-type equations. *Renewable Energy*, **1** (5), 811–814.
[54] Chiteka, K., and Enweremadu, C.C. (2016) Prediction of global horizontal solar irradiance in Zimbabwe using artificial neural networks. *Journal of Cleaner Production*, **135**, 701–711.
[55] Gómez, L.S.H., Ruiz-Muñoz, J.F., and Ruiz-Mendoza, B.J. (2022) Short-term forecasting of global solar irradiance in tropical environments with incomplete data. *Applied Energy*, **307**, 118192.
[56] Dhass, A.D., and Patel, D.R. (2022) Thermodynamic Analysis of Reflected Solar Radiation on Tilted PV Module in South India. *FME Transactions*, **50** (1), 158–167.
[57] Chanza, N., and Musakwa, W. (2022) Indigenous local observations and experiences can give useful indicators of climate change in data-deficient regions. *Journal of Environmental Studies and Sciences*.
[58] Sarr, A., Kebe, C.M.F., and Ndiaye, A. (2022) Validation of Helioclim-3 irradiance with ground observations in Senegal using four typical climatic zones. *Materials Today: Proceedings*, **51**, 1888–1895.
[59] Cai, H., Qin, W., Wang, L., Hu, B., and Zhang, M. (2021) Hourly clear-sky solar irradiance estimation in China: Model review and validations. *Solar Energy*, **226**, 468–482.
[60] Paul, D., De Michele, G., Najafi, B., and Avesani, S. (2022) Benchmarking clear sky and transposition models for solar irradiance estimation on vertical planes to facilitate glazed facade design. *Energy and Buildings*, **255**, 111622.
[61] Ghazouani, N., Bawadekji, A., El-Bary, A.A., Elewa, M.M., Becheikh, N., Alassaf, Y., and Hassan, G.E. (2022) Performance Evaluation of Temperature-Based Global Solar Radiation Models—Case Study: Arar City, KSA. *Sustainability*, **14** (1), 35.
[62] Hove, T., Manyumbu, E., and Rukweza, G. (2014) Developing an improved global solar radiation map for Zimbabwe through correlating long-term ground- and satellite-based monthly clearness index values. *Renewable Energy*, **63**, 687–697.
[63] Hove, T., and Göttsche, J. (1999) Mapping global, diffuse and beam solar radiation over Zimbabwe. *Renewable Energy*, **18** (4), 535–556.
[64] Makade, R.G., Chakrabarti, S., and Jamil, B. (2021) Development of global solar radiation models: A comprehensive review and statistical analysis for Indian regions. *Journal of Cleaner Production*, **293**, 126208.
[65] Bailey, M., Heinrich, D., and Kruczkiewicz, A. (2021) Climate Profiles of Countries in Southern Africa: Zimbabwe. *Red Cross Climate Centre*, 6.
[66] Bradley, K., Ingham, K., and Sanger, C.W. (2020) History, Map, Flag, Population, Capital, & Facts. *Britannica|Zimbabwe*.
[67] Rienecker, M.M., Suarez, M.J., Gelaro, R., Todling, R., Bacmeister, J., Liu, E., Bosilovich, M.G., Schubert, S.D., Takacs, L., Kim, G.-K., Bloom, S., Chen, J., Collins, D., Conaty, A., Silva, A. da, Gu, W., Joiner, J., Koster, R.D., Lucchesi, R., Molod, A., Owens, T., Pawson, S., Pegion, P., Redder, C.R., Reichle, R., Robertson, F.R., Ruddick, A.G., Sienkiewicz, M., and Woollen, J. (2011) MERRA: NASA's Modern-Era Retrospective Analysis for Research and Applications. *Journal of Climate*, **24** (14), 3624–3648.
[68] Westberg, D.J., Paul W. Stackhouse, J., Crawley, D.B., Hoell, J.M., Chandler, W.S., and Zhang, T. (2013) An analysis of NASA's MERRA meteorological data to supplement observational data for calculation of climatic design conditions. *ASHRAE Transactions*, **119** (2), 210–222.
[69] Shrestha, G.K., Pandey, B., Joshi, U., and Poudyal, K.N. (2021) Empirical model for estimation of global solar radiation at lowland region Biratnagar using satellite data. *BIBECHANA*, **18** (1), 193–200.
[70] Cebecauer, T., and Suri, M. (2016) Site-adaptation of satellite-based DNI and GHI time series: Overview and SolarGIS approach. *AIP Conference Proceedings*, **1734** (1), 150002.
[71] Fazelpour, F., Vafaeipour, M., Rahbari, O., and Valizadeh, M.H. (2013) Assessment of Solar Radiation Potential for Different Cities in Iran Using a Temperature-Based Method. *Sustainability in Energy and Buildings*, 199–208.
[72] Verhoelst, T., Granville, J., Hendrick, F., Köhler, U., Lerot, C., Pommereau, J.-P., Redondas, A., Van Roozendael, M., and Lambert, J.-C. (2015) Metrology of ground-based satellite validation: co-location mismatch and smoothing issues of total ozone comparisons. *Atmospheric Measurement Techniques*, **8** (12), 5039–5062.
[73] Zelenka, A., Perez, R., Seals, R., and Renné, D. (1999) Effective Accuracy of Satellite-Derived Hourly Irradiances. *Theor Appl Climatol*, **62** (3), 199–207.
[74] Yeom, J.-M., Seo, Y.-K., Kim, D.-S., and Han, K.-S. (2016) Solar Radiation Received by Slopes Using COMS Imagery, a Physically Based Radiation Model, and GLOBE. *Journal of Sensors*, **2016**, e4834579.
[75] Duffie, J.A., and Beckman, W.A. (2013) *Solar Engineering of Thermal Processes*, John Wiley & Sons.
[76] Gören, D., and Taylan, O. (2020) Quality Assessment of On-site Solar Radiation Data and Estimating Global Tilted Irradiation in Middle East Technical University Northern Cyprus Campus. *2020 2nd International Conference on Photovoltaic Science and Technologies (PVCon)*, 1–6.
[77] Almorox, J., Voyant, C., Bailek, N., Kuriqi, A., and Arnaldo, J.A. (2021) Total solar irradiance's effect on the performance of empirical models for estimating global solar radiation: An empirical-based review. *Energy*, **236**, 121486.
[78] Kumar, M., Kumar, P., Mukherjee, S., Priyadarshini, A., Biswas, S., and Namrata, K. (2022) Comparison And Validation Of Regression Model For Estimation Of Global Solar Radiation Using Python. *2022 IEEE International Students' Conference on Electrical, Electronics and Computer Science (SCEECS)*, 1–6.
[79] Fan, C., Chen, M., Wang, X., Wang, J., and Huang, B. (2021) A Review on Data Preprocessing

Techniques Toward Efficient and Reliable Knowledge Discovery From Building Operational Data. *Frontiers in Energy Research*, **9**.
[80] Yang, J., Rahardja, S., and Fränti, P. (2021) Mean-shift outlier detection and filtering. *Pattern Recognition*, **115**, 107874.
[81] Mabasa, B., Lysko, M.D., Tazvinga, H., Mulaudzi, S.T., Zwane, N., and Moloi, S.J. (2020) The Ångström–Prescott Regression Coefficients for Six Climatic Zones in South Africa. *Energies*, **13** (20), 5418.
[82] Uçkan, İ., and Khudhur, K.M. (2022) Improving of global solar radiation forecast by comparing other meteorological parameter models with sunshine duration models. *Environ Sci Pollut Res*.
[83] Balli, Ö. (2021) Estimating Global Solar Radiation from Empirical Models: An Application. *European Mechanical Science*, **5** (3), 135–147.
[84] Joshi, U., Karki, I.B., Chapagain, N.P., and Poudyal, K.N. (2021) Prediction of daily global solar radiation using different empirical models on the basis of meteorological parameters at Trans Himalaya Region, Nepal. *BIBECHANA*, **18** (1), 159–169.
[85] Li, F., Wang, R., Mao, L., Zhu, D., She, X., Guo, J., Lin, S., and Yang, Y. (2022) Evaluation of solar radiation models on vertical surface for building photovoltaic applications in Beijing. *IET Renewable Power Generation*, **n/a** (n/a).
[86] Zirebwa, F.S. (2014) An evaluation of the performance and subsequent calibration of two reference evapotranspiration estimation models for Gweru, Zimbabwe. 44–55.
[87] Hamza, B. (2021) Statistical Modelling Of Global Solar Radiation On Horizontal Surface Using Monthly Means Daily Sunshine Hours And Some Climatic Variables For Zamfara State, Nigeria. *International Journal of Advances in Scientific Research and Engineering*, **7** (5), 76–84.
[88] WMO (2018) *Guide to Instruments and Methods of Observation (WMO-No. 8)*, WMO, Geneva.
[89] Liu, Y., Tan, Q., and Pan, T. (2019) Determining the Parameters of the Ångström-Prescott Model for Estimating Solar Radiation in Different Regions of China: Calibration and Modeling. *Earth and Space Science*, **6** (10), 1976–1986.
[90] Salima, G., and Chavula, G.M.S. (2012) Determining Angstrom Constants for Estimating Solar Radiation in Malawi. *International Journal of Geosciences*, **03** (02), 391.
[91] Fernando, D.M.Z., Calca, M.V.C., Raniero, M.R., and Pai, A.D. (2019) Irradiação Solar Global Para Cidade De Maputo - Moçabique: Evolução Temporal Das Medidas e Modelagem Estatística. *Energia na Agricultura*, **34** (01), 82–93.
[92] Mulaudzi, T.S. (2019) Evaluation of the regression coefficients for South Africa from solar radiation data.